

Superconductivity in layered Oxychalcogenide $\text{La}_2\text{O}_2\text{Bi}_3\text{AgS}_6$

Rajveer Jha^{1,*}, Yosuke Goto¹, Ryuji Higashinaka¹, Tatsuma D. Matsuda¹, Yuji Aoki¹, and
Yoshikazu Mizuguchi^{1, †}

¹Department of Physics, Tokyo Metropolitan University, 1-1 Minami-osawa, Hachioji, Tokyo
192-0397, Japan

Abstract:

We report the superconductivity in layered oxychalcogenide $\text{La}_2\text{O}_2\text{Bi}_3\text{AgS}_6$ compound. The $\text{La}_2\text{O}_2\text{Bi}_3\text{AgS}_6$ compound has been reported recently by our group, which has a tetragonal structure with the space group $P4/nmm$. The crystal structure of $\text{La}_2\text{O}_2\text{Bi}_3\text{AgS}_6$ can be regarded as alternate stacks of LaOBiS_2 -type layer and rock-salt-type $(\text{Bi,Ag})\text{S}$ layer. We measured low-temperature electrical resistivity and observed superconductivity at 0.5 K. The observation of superconductivity in the $\text{La}_2\text{O}_2\text{Bi}_3\text{AgS}_6$ should provide us with the successful strategy for developing new superconducting phases by the insertion of a rock-salt-type chalcogenide layer into the van der Waals gap of BiS_2 -based layered compound like LaOBiS_2 .

Keywords: BiS_2 -based superconductors; layered superconductor; electrical resistivity; adiabatic demagnetization refrigerators (ADR)

E-mail for corresponding authors: *rajveerjha@gmail.com, †mizugu@tmu.ac.jp

The discovery of BiS₂-based superconductors made a huge interest in the scientific community [1,2]. In this progress several new materials possessing the bismuth chalcogenides [BiCh₂ (Ch=S, Se)] layers have been designed [1-10]. Firstly, the superconductivity has been reported in Bi₄O₄S₃ layered compound with a transition temperature (T_c) of 4.5 K [1,3]. Later, other BiS₂-based superconductors REO_{1-x}F_xBiS₂ (RE = La, Ce, Nd, Yb, Pr) and Sr_{1-x}La_xFBiS₂ were discovered after Bi₄O₄S₃ [1-11]. So far, the superconductivity in the BiS₂ based compounds has been reported to be induced via charge carrier doping into BiS₂ layers for the REO_{1-x}F_xBiS₂ and Sr_{1-x}RE_xFBiS₂ compounds [3-11]. These superconductors are very sensitive to the external hydrostatic pressure and the highest T_c above 10 K was achieved for LaO_{0.5}F_{0.5}BiS₂ and Sr_{1-x}RE_xFBiS₂ (RE = La, Ce, Nd, Pr, Sm) compounds [12-16].

Recently, new layered oxysulfide LaOPbBiS₃ has been reported by Y.-L. Sun *et. al* [17]. They proposed that LaOPbBiS₃ compound is a narrow gap semiconductor with an activation energy of ~17 meV, which suggested that LaOPbBiS₃ and its derivatives may be promising for thermoelectric applications [17]. After careful structural analysis for the LaOBiPbS₃ phase [18], we have proposed a material design strategy focusing on the van der Waals gaps between the two BiCh₂ layers. The van der Waals gaps of LaOBiS₂ can be filled by inserting some rock salt layers composed of M₂S₂ [M = Pb, Bi] [18], which results in the formation of La₂O₂M₄S₆-type compounds. Later on, Y. Hijikata *et al.* reported the synthesis of La₂O₂Bi₃AgS₆ compound [19]. The structure of La₂O₂Bi₃AgS₆ is similar to LaOBiPbS₃, but the interlayer bond (M2-S1 bond) in La₂O₂Bi₃AgS₆ is shorter than that of LaOBiPbS₃. The electrical conductivity and carrier concentration of La₂O₂Bi₃AgS₆ are higher than those of LaOBiPbS₃ and LaOBiS₂, possibly due to the shorter interlayer bonds and/or chemical pressure effect with compressed *a*-axis [19]. Our previous electrical resistivity and magnetization measurements showed no signature of a superconducting transition down to 2 K [19].

Here, we measured the electrical resistivity of La₂O₂Bi₃AgS₆ down to 0.1 K using an adiabatic demagnetization refrigerator (ADR) system. We observed superconductivity in La₂O₂Bi₃AgS₆ compound at $T_c^{\text{zero}} = 0.5$ K. This is the first observation of superconductivity among La₂O₂M₄S₆-type compounds.

The polycrystalline sample of La₂O₂Bi₃AgS₆ was prepared by a solid-state reaction method. Powders of Bi₂O₃ (99.9%), La₂S₃ (99.9%), and AgO (99.9%) and grains of Bi (99.999%) and S

(99.99%) with a nominal composition of $\text{La}_2\text{O}_2\text{Bi}_3\text{AgS}_6$ were mixed in a pestle and mortar, pelletized, sealed in an evacuated quartz tube, and heated at 720 °C for 15 h. The obtained sample was reground for homogeneity, pelletized, and heated at 720 °C for 15 h. The phase purity of the prepared sample and the optimal annealing conditions were examined using laboratory X-ray diffraction (XRD) with Cu-K_α radiation. The crystal structure parameters were refined using the Rietveld method with RIETAN-FP [20]. Schematic image of the crystal structure were drawn using VESTA (see the inset of Fig. 1) [21]. The electrical resistivity down to $T = 0.1$ K was measured by four probe technique using adiabatic demagnetization refrigerator (ADR) system on the Physical Property measurement system (PPMS: Quantum Design).

Figure 1 shows the room temperature XRD pattern of $\text{La}_2\text{O}_2\text{Bi}_3\text{AgS}_6$ compound. The $\text{La}_2\text{O}_2\text{Bi}_3\text{AgS}_6$ compound crystallized in the tetragonal structure with the space group of $P4/nmm$, which is composed of stacked $[\text{M}_4\text{S}_6]$ layers and fluorite-type $[\text{La}_2\text{O}_2]$ layers. No impurity peak has been observed, and all the observed peaks are well indexed to the main phase of $\text{La}_2\text{O}_2\text{Bi}_3\text{AgS}_6$ compound, which is comparable to the previous study [19]. The estimated lattice parameters are $a = 4.0568(1)$ Å and $c = 19.348(1)$ Å. The crystal structure of $\text{La}_2\text{O}_2\text{Bi}_3\text{AgS}_6$ compound is shown in the inset of Fig. 1, in which chalcogenide layers of $(\text{BiAg})\text{S}$ and $\text{LaO}(\text{BiAg})\text{S}_2$ are alternately stacking.

Figure 2 shows the temperature dependence of electrical resistivity $[\rho(T)]$ from 300 to 0.1 K. The overall behavior of the normal state electrical resistivity is metallic. The lower resistivity in comparison with previous report might be due to the smaller lattice parameters for this sample. The smaller lattice parameter c can make the shorter interlayer M1-S3 bonding. Due to the smaller lattice parameter a the in-plane M1-S1 bonding becomes shorter, which is preferable for metallic conductivity [22]. We have analyzed the composition of the sample using energy dispersive x-ray spectroscopy (EDX) and found slightly high concentration of Ag in the present sample in comparison with the previous sample [19]. The smaller lattice parameters might be due to the excess Ag concentration in the present sample.

Notably, we observed a broad hump in the $\rho(T)$ curve below $T^* \sim 180$ K, which is quite similar to the hump observed in the $\rho(T)$ curve below ~ 280 K for the EuFBiS_2 compound, which shows superconductivity at 0.3 K [23]. The origin of the hump in the $\rho(T)$ curve was proposed as the charge density wave (CDW) transition in EuFBiS_2 . From the analogy, we assume that the anomaly is caused by a CDW transition.

The resistivity starts to deviate from the normal state value below the temperature 2.5 K and becomes zero at 0.5 K [see the inset of Fig. 2], which suggests the emergence of superconductivity in the $\text{La}_2\text{O}_2\text{Bi}_3\text{AgS}_6$ compound. As mentioned above, the anomaly at T^* may be related to a CDW transition. Therefore, it is expected that some part of the Fermi surface disappears in the CDW state and the superconductivity develops on the remaining part. With the $\text{La}_2\text{O}_2\text{Bi}_3\text{AgS}_6$ and related $\text{La}_2\text{O}_2\text{M}_4\text{S}_6$ systems, we may be able to discuss the universal relationship between superconductivity and CDW in the BiCh_2 -based compounds.

Furthermore, there is another notable characteristics in the $\text{La}_2\text{O}_2\text{M}_4\text{S}_6$ system. According to the band calculations for LaOBiPbS_3 [18], the valence bands just below the Fermi energy (E_F) are mainly composed of S-3p orbitals of the S3 site (see the inset of Fig. 1) in the M_2S_2 layer. This is different from the case of the typical BiS_2 -based compounds in which the valence bands just below E_F are composed of S-3p orbitals of the in-plane S1 site. The similar situation is expected for $\text{La}_2\text{O}_2\text{Bi}_3\text{AgS}_6$ compound: the valence bands near E_F would be composed of S-3p bands of the rock-salt type (Bi,Ag)S layer. Therefore, the superconductivity states in $\text{La}_2\text{O}_2\text{Bi}_3\text{AgS}_6$ may be different from those of the typical BiS_2 -based superconductors because of the difference in the electronic states near E_F . We expect that the discovery of the superconductivity in $\text{La}_2\text{O}_2\text{Bi}_3\text{AgS}_6$ will extend the field of layered bismuth chalcogenide superconductors.

In conclusion, we reported the observation of superconductivity ($T_c^{\text{zero}} = 0.5$ K) in the polycrystalline sample of layered oxychalcogenide $\text{La}_2\text{O}_2\text{Bi}_3\text{AgS}_6$. In the temperature dependence of resistivity, an anomaly possibly related to the CDW transition ($T^* \sim 180$ K) is observed. The $\text{La}_2\text{O}_2\text{Bi}_3\text{AgS}_6$ and related $\text{La}_2\text{O}_2\text{M}_4\text{S}_6$ systems will be useful to discuss the universal relationship between superconductivity and CDW states and to develop new CDW-related superconductors.

Acknowledgments:

We gratefully appreciate K. Matsubayashi and Y. Yuan of University of Electrocommunication and O. Miura and Y. Hijikata of Tokyo Metropolitan University for fruitful discussions. This work was financially supported by grants in Aid for Scientific Research (KAKENHI) (Grant Nos. 15H05886, 15H05884, 16H04493, 17K19058, 16K05454, and 15H03693)

Reference:

1. Y. Mizuguchi, H. Fujihisa, Y. Gotoh, K. Suzuki, H. Usui, K. Kuroki, S. Demura, Y. Takano, H. Izawa, and O. Miura, *Phys. Rev. B* **86**, 220510 (2012).
2. Y. Mizuguchi, S. Demura, K. Deguchi, Y. Takano, H. Fujihisa, Y. Gotoh, H. Izawa, and O. Miura, *J. Phys. Soc. Jpn.* **81**, 114725 (2012).
3. S. K. Singh, A. Kumar, B. Gahtori, S. Kirtan, G. Sharma, S. Patnaik, and V. P. S. Awana, *J. Am. Chem. Soc.* **134**, 16504 (2012).
4. S. Demura, Y. Mizuguchi, K. Deguchi, H. Okazaki, H. Hara, T. Watanabe, S. J. Denholme, M. Fujioka, T. Ozaki, H. Fujihisa, Y. Gotoh, O. Miura, T. Yamaguchi, H. Takeya, Y. Takano, *J. Phys. Soc. Jpn.* **82**, 033708 (2013).
5. R. Jha, A. Kumar, S. K. Singh, V. P. S. Awana, *J. Supercond. Nov. Magn.* **26**, 499 (2013)
6. J. Xing, S. Li, X. Ding, H. Yang, H.H. Wen, *Phys. Rev. B* **86**, 214518 (2012).
7. D. Yazici, K. Huang, B. D. White, A. H Chang, A. J. Friedman, M. B. Maple, *Philos. Mag.* **93**, 673 (2012).
8. D. Yazici, K. Huang, B. D. White, I. Jeon, V. W. Burnett, A.J. Friedman, I. K. Lum, M. Nallaiyan, S. Spagna, M. B. Maple, *Phys. Rev. B* **87**, 174512 (2013).
9. A. Krzton-Maziopa, Z. Guguchia, E. Pomjakushina, V. Pomjakushin, R. Khasanov, H. Luetkens, P. Biswas, A. Amato, H. Keller, K. Conder, *J. Phys.: Condens. Matter* **26**, 215702 (2014).
10. Y. Mizuguchi, A. Omachi, Y. Goto, Y. Kamihara, M. Matoba, T. Hiroi, J. Kajitani, O. Miura, *J. Appl. Phys.* **116**, 163915 (2014).
11. X. Lin, X. Ni, B. Chen, X. Xu, X. Yang, J. Dai, Y. Li, X. Yang, Y. Luo, Q. Tao, G. Cao, Z. Xu, *Phys. Rev. B* **87**, 020504 (2013).
12. H. Kotegawa, Y. Tomita, H. Tou, H. Izawa, Y. Mizuguchi, O. Miura, S. Demura, K. Deguchi, Y. Takano, *J. Phys. Soc. Jpn.* **81**, 103702 (2012).
13. C. T. Wolowiec, D. Yazici, B. D. White, K. Huang, M. B. Maple, *Phys. Rev. B* **88**, 064503 (2013).
14. C. T. Wolowiec, B. D. White, I. Jeon, D. Yazici, K. Huang, M. B. Maple, *J. Phys.: Condens. Matter* **25**, 422201 (2013).
15. R. Jha, B. Tiwari, V. P. S. Awana, *J. Phys. Soc. Jpn.* **83**, 063707 (2014).

16. R. Jha, B. Tiwari, V. P. S. Awana, J. Appl. Phys. **117**, 013901 (2015).
17. Y.-L. Sun, A. Ablimit, H.-F. Zhai, J.-K. Bao, Z.-T. Tang, X.-B. Wang, N.-L. Wang, C.-M. Feng, and G.-H. Cao, Inorg. Chem. **53**, 11125 (2014).
18. Y. Mizuguchi, Y. Hijikata, T. Abe, C. Moriyoshi, Y. Kuroiwa, Y. Goto, A. Miura, S. Lee, S. Torii, T. Kamiyama, C. H. Lee, M. Ochi, K. Kuroki, EPL **119** 26002 (2017).
19. Y. Hijikata, T. Abe, C. Moriyoshi, Y. Kuroiwa, Y. Goto, A. Miura, K. Tadanaga, Y. Wang, O. Miura, and Y. Mizuguchi, J. Phys. Soc. Jpn. **86**, 124802 (2017).
20. F. Izumi and K. Momma, Solid State Phenom. **130**, 15 (2007).
21. K. Momma and F. Izumi, J. Appl. Crystallogr. **41**, 653 (2008).
22. Y. Mizuguchi, A. Miura, J. Kajitani, T. Hiroi, O. Miura, K. Tadanaga, N. Kumada, E. Magome, C. Moriyoshi, Y. Kuroiwa, Sci. Rep. **5**, 14968 (2015).
23. H.-F. Zhai, Z.-T. Tang, H. Jiang, K. Xu, K. Zhang, P. Zhang, J.-K. Bao, Y.-L. Sun, W.-H. Jiao, I. Nowik, I. Felner, Y.-K. Li, X.-F. Xu, Q. Tao, C.-M. Feng, Z.-A. Xu, and G.-H. Cao, Phys. Rev. B **90**, 064518 (2014).

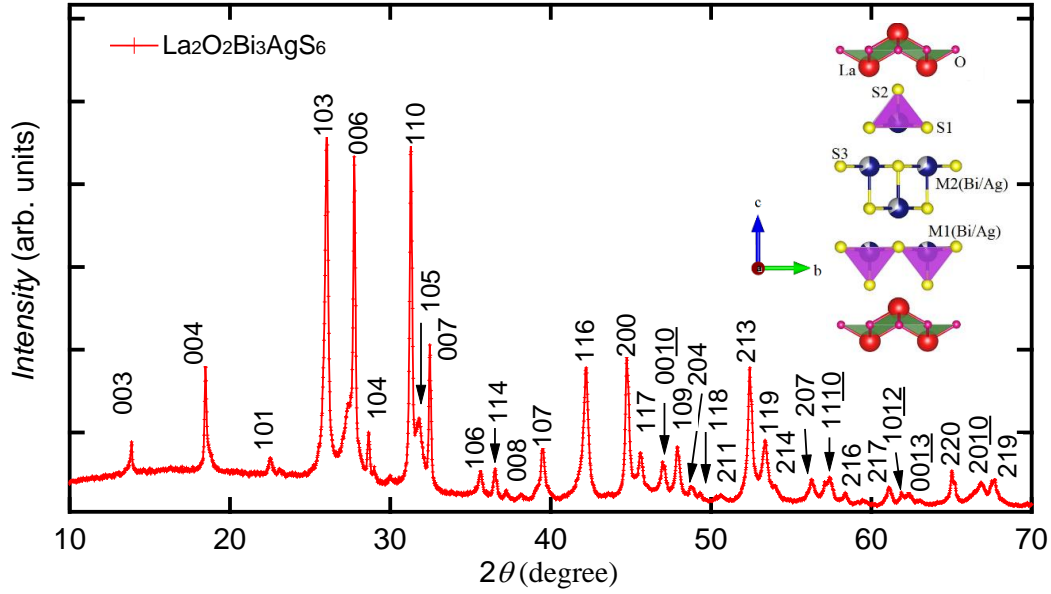


Fig. 1: (color online) The room temperature XRD pattern of $\text{La}_2\text{O}_2\text{Bi}_3\text{AgS}_6$ compound. The numbers in the XRD pattern are Miller indices. Inset is the schematic unit cell obtained by a refinement using the Rietveld method with RIETAN-FP [20]

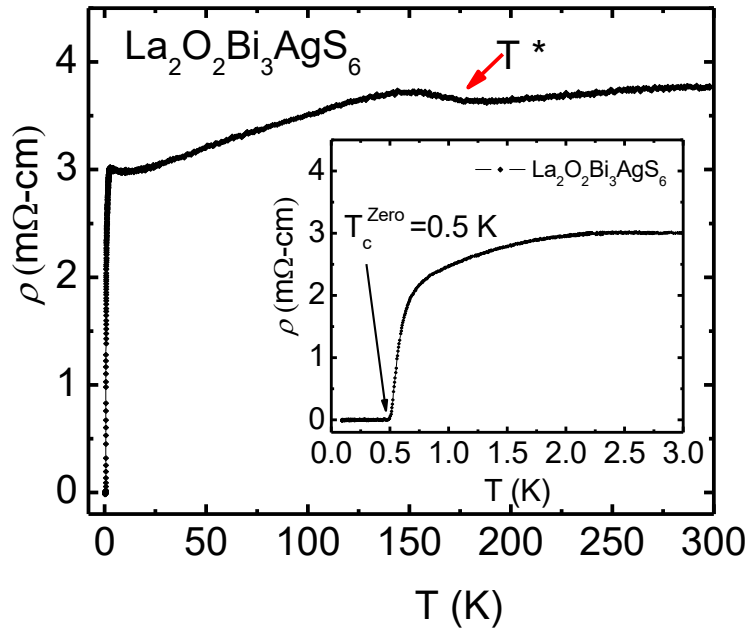


Fig. 2: (color online) The temperature dependence of electrical resistivity down to 0.1 K for the $\text{La}_2\text{O}_2\text{Bi}_3\text{AgS}_6$ compound. A hump structure appearing in the $\rho(T)$ curve is denoted by T^* . Inset is the $\rho(T)$ curve in the temperature range 3.0 to 0.1 K.